Spin-Resolved Photoemission from Xe on Pd(111) in the Dilute Phase: The Model Case of Singly Adsorbed Atoms

B. Vogt, B. Kessler, N. Müller, G. Schönhense, B. Schmiedeskamp, and U. Heinzmann Fakultät für Physik, Universität Bielefeld, D-4800 Bielefeld, Federal Republic of Germany and Fritz-Haber-Institut der Max-Planck-Gesellschaft, D-1000 Berlin 33, Federal Republic of Germany (Received 10 December 1990)

Xe adsorbed on Pd(111) in the dilute phase, in the $(\sqrt{3} \times \sqrt{3})R30^{\circ}$, and in the $(\sqrt{7} \times \sqrt{7})R19.2^{\circ}$ structure has been studied by spin-resolved photoemission with normally incident circularly polarized light and for normal electron emission. Similar to the free atomic case, no splitting was observed for the dilute phase in the peak corresponding to the $p_{3/2}$ hole state. Subthreshold electronic resonances were found for the two ordered layers, but could not be detected for the dilute phase. Consequences regarding the splitting mechanism and the excitation and emission processes for the resonances are discussed.

PACS numbers: 71.70.Ej, 79.60.Gs

The valence levels of Xe adsorbates in the monolayer regime have been studied by photoemission [1-4] and spin-resolved photoemission [5-9]. When a photon ionizes a free Xe atom in the outer shell, a Xe⁺ 5p⁵(²P_{1/2}) or Xe⁺ 5p⁵(²P_{3/2}) final ionic state, called the $p_{1/2}$ or $p_{3/2}$ hole state, is created. For adsorbates, a broadening of the peak corresponding to the $p_{3/2}$ hole state was observed [1]. It was interpreted as a lifting of the $|m_j|$ degeneracy of the $p_{3/2}$ hole state and a splitting into its $|m_j| = \frac{1}{2}$ and $|m_j| = \frac{3}{2}$ sublevels. Different theories about the physical nature of the splitting [1-4,10-12] have been stated, differing in the energetic ordering of the $|m_j| = \frac{1}{2}$ and $|m_j| = \frac{3}{2}$ sublevels.

A splitting due to substrate-induced screening of the ionic hole state [10,11] or to the formation of moleculelike orbitals [12] results in an ordering with the $|m_i| = \frac{3}{2}$ sublevel at higher binding energy. A splitting caused by the crystal field of the substrate [1] or lateral interactions, i.e., band formation [2-4], results, however, in an ordering with the $|m_i| = \frac{3}{2}$ sublevel at lower binding energy. For Xe monolayers on Pt(111), Ir(111), and graphite it was shown by spin-resolved photoemission [5,7] that the $|m_i| = \frac{3}{2}$ sublevel of the hole state corresponds to lower binding energy. This fact ruled out several models [10-12]. In addition, the observed magnitude of the splitting cannot be explained by the model presented in Ref. [1]. Only the assumption that the splitting is due to lateral interactions [2-4] is compatible with the results in Refs. [5] and [7]. However, up to now only the close-packed-hexagonal layer and the commensurate $(\sqrt{3} \times \sqrt{3})R30^{\circ}$ layer have been investigated.

At certain photon energies of the incident light, well below the onset of direct photoemission, highly spin-polarized electrons could be detected at the vacuum level [6,7]. The spin marking of these "subthreshold resonances" allowed an assignment of the electronic states involved in analogy to atomic transitions of the form $5p \rightarrow 6s$ (the Xe 6s level lies below the vacuum level). As the mechanism of how the electrons leave the Xe adsorbate, a Penning-type emission process at the adsorbate-substrate interface has been proposed [6,7].

For the interpretation of both the splitting of the $p_{3/2}$ hole state and the electron emission process for the resonances, it is of great interest to study the ideal system of a single Xe adatom: As the valence orbital overlap, which dominates the splitting in the monolayer regime, is absent in this case, one can expect to get information about the possible remaining splitting mechanisms. Furthermore, the proposed excitation and emission processes for the resonances should in principle also be possible for a single Xe adatom on the surface. Hence the search for subthreshold resonances in such a system would be a sensitive test of the proposed models. It is the purpose of this Letter to present and discuss experimental data for the model case of singly adsorbed Xe atoms.

Pd was chosen as a substrate because Xe is known to form a dilute phase (also called 2D gas phase) on Pd(100) up to high coverages below one layer [13,14]. The existence of the dilute phase is correlated with and attributed to a high dipole moment [14,15] of the Xe atoms on Pd(100) and to high adsorption energies [13,15-17]. As the dipole moment of Xe on Pd(111) is even higher than on Pd(100) [17], we also expect a dilute phase on the (111) surface up to high coverages. For this dilute phase we hope to find the model case of singly adsorbed Xe atoms.

The experiments were performed at the 6.5-m normalincidence vacuum-ultraviolet monochromator [18] at BESSY. The apparatus used for the measurements has been described previously [19]. All photoemission data were obtained for normal incidence of the circularly polarized synchrotron radiation and normal photoelectron emission. The photoelectrons were analyzed with respect to their kinetic energy by a 180° spherical field spectrometer [20]. The overall energy resolution (electrons and photons) was better than 150 meV at an angular resolution of $\pm 3^{\circ}$ up to $\pm 10^{\circ}$ depending on the photon energy. The analysis of the spin polarization of the electrons was performed by Mott scattering. Experimental asymmetries were eliminated by changing the light helicity from σ^+ to σ^- . The Pd(111) crystal was mounted on top of a liquid-He-cooled manipulator. The surface normal of the crystal coincided within 0.5° with the [111]

direction and within 0.3° with the light direction. For the preparation of a clean surface cycles of Ar⁺ or Ne⁺ bombardment, heating in oxygen, and heating up to 1000 K were performed. The surface contamination was controlled by Auger electron spectroscopy. For carbon contamination CO desorption spectroscopy was used, since the Auger signal of carbon coincides with a Pd signal. The surface structure was monitored by LEED.

The experiment results are presented in Fig. 1. In the center and right-hand panels, LEED patterns and structure models for the Xe adsorbates are shown; the corresponding photoelectron intensity spectra for hv=11 eV are given in the left-hand panel. Up to the maximum Xe coverage at temperatures of 80 ± 5 K the LEED pattern of Fig. 1(a) occurs. Only spots at the positions of the spots obtained for a clean Pd(111) crystal are visible; no extra spots can be seen, indicating that there is no lateral ordering in the adsorbate. This structure, called the dilute phase, occurs up to coverages which show 80% of the work-function change of the complete $(\sqrt{3} \times \sqrt{3})R30^{\circ}$ layer (further Xe does not adsorb at these temperatures) as could be shown by a phase transition to the $(\sqrt{3} \times \sqrt{3})R30^{\circ}$ structure. This phase transition was obtained only by lowering the temperature and without dosing more Xe. The Xe coverage of the dilute phase is thus connected to the coverage of the $(\sqrt{3} \times \sqrt{3})R30^{\circ}$ structure for which a complete layer is defined to have the coverage 1. The photoemission spectra of the dilute phase are identical to the one presented in Fig. 1; only the absolute intensity values scale with coverage between 0.2 and 0.8 layer. The spin-resolved photoemission spectrum of

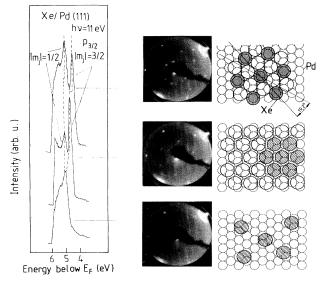


FIG. 1. Photoelectron intensity spectra of Xe/Pd(111) taken at hv=11 eV (left-hand panel), LEED patterns (center panels), and compatible structures (right-hand panels) for (a) the dilute phase, (b) the $(\sqrt{3} \times \sqrt{3})R30^{\circ}$ structure, and (c) the $(\sqrt{7} \times \sqrt{7})R19.2^{\circ}$ structure.

Fig. 2 was taken at 0.5 layer. The LEED pattern, the structure model, and the photoelectron intensity spectrum corresponding to the $(\sqrt{3} \times \sqrt{3})R30^{\circ}$ structure obtained at 65 ± 5 K are presented in Fig. 1(b). In contrast to the substrates Ir(111) and Pt(111) [7,8,21], further Xe exposure and decrease in temperature lead to a commensurate structure until a second layer adsorbs. The LEED pattern of this structure taken at 50 ± 5 K is presented in Fig. 1(c). A structure model is proposed in the right-hand part of Fig. 1(c). It is a close-packed layer with a $(\sqrt{7} \times 7)R19.2^{\circ}$ buckled coincidence structure. This buckled structure results in a projection of the Xe-Xe distance of 4.2 ± 0.05 Å, close to the Xe bulk value of 4.34 Å. Two domains occur, rotated by $\pm 19.2^{\circ}$ with respect to the underlying Pd substrate.

From the corresponding photoemission spectra in Fig. 1, obtained for a photon energy of hv = 11 eV, we get information regarding the splitting of the $p_{3/2}$ hole state. We find a splitting for the $(\sqrt{7} \times \sqrt{7})R19.2^{\circ}$ structure of 0.58 ± 0.03 eV and a considerably smaller splitting for the $(\sqrt{3} \times \sqrt{3})R30^{\circ}$ adsorbate structure of 0.4 ± 0.03 eV. For the two ordered structures we find, by spin-resolved measurements, the $|m_j| = \frac{3}{2}$ sublevel of the hole state at a lower binding energy than the $|m_i| = \frac{1}{2}$ sublevel. In analogy to [5] and [7] we can thus conclude that the splitting for the two ordered structures of Xe/Pd(111) is also due to the lateral Xe-Xe interaction. For the dilute phase we observe only a broad peak in Fig. 1 which shows no splitting. Information as to whether the $p_{3/2}$ hole state is split or not can thus not be obtained from this spectrum.

More information about the existence of a possible splitting can be expected from spin-resolved photoemission experiments. If the peak is split [7], the preferential spin direction of the photoelectrons corresponding to the $p_{3/2} |m_i| = \frac{1}{2}$ hole state should be parallel to the photon spin (polarization P > 0) and the preferential spin direction corresponding to the $p_{3/2} |m_i| = \frac{3}{2}$ hole state should be antiparallel to the photon spin (polarization P < 0) for our geometry and photon energies (see, e.g., [7]). The change of sign of the spin polarization in the $p_{3/2}$ peak thus allows a precise determination of the size of the $|m_i|$ splitting and, via the sequence of the spin-polarization signs, a determination of the sublevel ordering. A spinresolved photoemission spectrum for the dilute phase is presented in Fig. 2. The total intensity I (upper curve) is separated into the partial intensities I_+ and I_- of the electrons totally polarized parallel and antiparallel to the photon spin, respectively, by means of the measured spin polarization P and the equations $I_{+}=I/2(1+P)$ and $I_{-}=I/2(1-P)$. Within the experimental uncertainty of about 100 meV we measure no splitting of the $p_{3/2}$ peak for the dilute phase. The polarization for this peak is nearly -50% (in agreement with the value measured for a free Xe atom [22]). Although the electronic structure, the band structure, and the spin-orbit splitting vary for

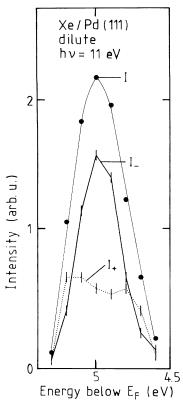


FIG. 2. Spin-resolved photoelectron spectrum at hv = 11 eV for the dilute phase.

different materials, it is worth noting that for disordered Ge with lateral interaction, zero spin polarization was measured, in contrast to polycrystalline Ge [23]. The spin-polarization value measured for the dilute phase is not zero as for disordered Ge with lateral interaction or as for ordered Xe, but -50% as for a free Xe atom [22]. All of this indicates that the Xe atoms are singly adsorbed on Pd(111) in the dilute phase.

Considering the facts that the splitting of the $p_{3/2}$ peak is smaller than 100 meV for the dilute phase, that for all ordered Xe phases studied up to now by spin-resolved photoemission splittings between 0.4 and 0.6 eV were found, and that in all cases the $|m_i| = \frac{3}{2}$ level was found at lower binding energy, we draw the conclusion that the mechanisms described in Refs. [1,10-12], which are not based on a lateral Xe-Xe interaction, yield a very small contribution to the splitting of the $p_{3/2}$ peak. This conclusion is supported by the finding that by lowering the temperature $(\sqrt{3} \times \sqrt{3}) R30^{\circ}$ islands, for which a splitting of the $p_{3/2}$ hole state of 0.4 eV was observed, can be obtained directly from the dilute phase. Even if the broad structure in I_+ was explained as a superposition of several peaks, this would not result in a splitting comparable to that of the ordered phases.

Measurements of the subthreshold resonances for the different phases are presented in Fig. 3. We varied the photon energy and measured the intensity *I* and spin po-

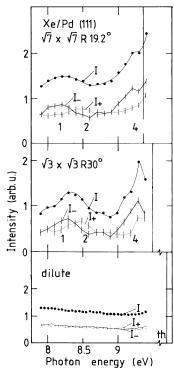


FIG. 3. Subthreshold resonances for three phases of Xe/Pd(111): Constant-final-state spectra taken just above the vacuum level for the $(\sqrt{7} \times \sqrt{7})R19.2^{\circ}$ structure (upper part), the $(\sqrt{3} \times \sqrt{3})R30^{\circ}$ structure (middle part), and the dilute phase (lower part).

larization P of the electrons just above the vacuum level (their kinetic energy was 0.15 eV). The intensity I is again separated into I_+ and I_- and we find three peaks labeled 1, 2, and 4 (adopting the labeling of Refs. [6-8]) for the two ordered phases of Xe on Pd(111). These are displayed in the two upper panels of Fig. 3. The peaks occur at about the same photon energies as those obtained earlier on Pt(111) [6,7] and Ir(111) [8] and are also in fair agreement with $5p \rightarrow 6s$ excitation energies of the free Xe atom. The results fit quite well into the model given in Refs. [6-8], which describes the observed process as a combination of atomiclike excitation and Penning-type electron emission.

For the dilute phase we find, however, no structure in the total intensity and the partial intensities $(I_+ \approx I_-)$ of the constant-final-state spectrum just above the vacuum level, as can be seen from the lowest panel in Fig. 3. It thus seems that the resonances occur only when a well-ordered Xe overlayer is present.

The experimental result of existing subthreshold resonances for two-dimensional systems and missing resonances for a dilute phase in the submonolayer range is similar to former experimental results [24-26] obtained for excitonic states of rare gases. Optical measurements on rare-gas solids proved the existence of surface excitons [24], which are confined to one or two layers at the

sample-vacuum boundary. In fluorescence measurements on rare-gas clusters [25], surface excitons were detected for large $(N \ge 200)$ and intermediate $(50 \le N \le 200)$ clusters; for small clusters $(N \le 30)$ absorption structures could also be detected. In reflectance measurements of submonolayer Xe on several polycrystalline metal surfaces [26], excitonic states were observed above one monolayer, but could not be detected at submonolayer coverage. This was interpreted as being due to charge transfer to the substrate (perhaps tunneling of the excited 6s electron into an empty state above E_F of the metal) which prevents detection of the excited state.

The additional information of the spin marking of the electrons in our experiments gives further hints regarding the nature of the subthreshold resonances in our spectra. If the whole process can be described as a two-step process, i.e., a combination of photoexcitation with optical spin orientation and subsequent electron emission, the spin marking of the emitted electrons and the energetic position support the model that the excitation is derived from the Xe $5p \rightarrow 6s$ transition [6,7]. The existence of a transition from the 5p level into an empty and broadened 6s level also appears to be necessary to understand dipole moment and adsorption energy measurements on Xe/ Pd(111) [17]. For small Kr clusters ($N \le 30$) [25], transitions like this could be observed. A decay of this excited state via electron emission (with preferential spin direction) could not be observed without ordered Xe islands in our experiments. Possible explanations for this finding are that either the excitation process is excitonic rather than free-atom-like and can thus occur only in an ordered overlayer or the electron emission process demands Xe neighbors.

In summary, we observe three structures of Xe on Pd(111): the dilute phase and the two ordered $(\sqrt{3} \times \sqrt{3})R30^{\circ}$ and $(\sqrt{7} \times \sqrt{7})R19.2^{\circ}$ structures. The dilute phase can be well described by the model of singly adsorbed Xe atoms, as a comparison of the emission from the dilute phase with that from a free Xe atom and the ordered systems shows.

While the $p_{3/2}$ hole state shows a splitting of 0.4 and 0.58 eV for the two ordered phases with the $|m_j| = \frac{3}{2}$ level at lower binding energy, no splitting larger than 0.1 eV is found for the dilute phase. It can thus be concluded that only one of the splitting mechanisms discussed in the literature, namely, the mechanism which is based on a lateral Xe-Xe interaction, contributes considerably to the splitting.

Subthreshold resonances which have been studied earlier for various ordered Xe structures on different substrates and which were described in a model with atomic-like excitation and subsequent Penning-type electron emission are not observed for the dilute phase. A model for these resonances thus cannot be based on a singly adsorbed Xe atom. Well-ordered Xe adatom islands seem to be an essential part of either the excitation or the emission process.

We would like to thank the BESSY staff for their support. This work was financially supported by the BMFT (Sonderforschungsbereich No. 5431).

- [1] B. J. Waclawski and J. F. Herbst, Phys. Rev. Lett. 35, 1594 (1975).
- [2] K. Horn, M. Scheffler, and A. M. Bradshaw, Phys. Rev. Lett. 41, 822 (1978).
- [3] M. Scheffler, K. Horn, A. M. Bradshaw, and K. Kambe, Surf. Sci. 80, 69 (1979).
- [4] K. Horn, C. Mariani, and L. Cramer, Surf. Sci. 117, 376 (1982).
- [5] G. Schönhense, A. Eyers, U. Friess, F. Schäfers, and U. Heinzmann, Phys. Rev. Lett. 54, 547 (1985).
- [6] G. Schönhense, A. Eyers, and U. Heinzmann, Phys. Rev. Lett. 56, 512 (1986).
- [7] G. Schönhense, Appl. Phys. A 41, 39 (1986).
- [8] G. Schönhense, B. Kessler, N. Müller, B. Schmiedeskamp, and U. Heinzmann, Phys. Scr. 35, 541 (1987).
- [9] U. Heinzmann, Phys. Scr. T 17, 77 (1987).
- [10] J. A. D. Matthew and M. G. Devey, J. Phys. C 9, L413 (1976).
- [11] P. R. Antoniewicz, Phys. Rev. Lett. 38, 374 (1977).
- [12] S.-I. Ishi and Y. Ohno, J. Electron. Spectrosc. Relat. Phenom. 33, 85 (1984).
- [13] A. Jablonski, S. Eder, K. Markert, and K. Wandelt, J. Vac. Sci. Technol. A 4, 1510 (1986).
- [14] R. Miranda, S. Daiser, K. Wandelt, and G. Ertl, Surf. Sci. 131, 61 (1983).
- [15] S. Eder, K. Markert, A. Jablonski, and K. Wandelt, Ber. Bunsenges. Phys. Chem. 90, 225 (1985).
- [16] K. Wandelt and J. E. Hulse, J. Chem. Phys. 80, 1340 (1984).
- [17] K. Wandelt and B. Gumhalter, Surf. Sci. 140, 355 (1984).
- [18] F. Schäfers, W. Peatman, A. Eyers, Ch. Heckenkamp, G. Schönhense, and U. Heinzmann, Rev. Sci. Instrum. 57, 1032 (1986).
- [19] A. Eyers, F. Schäfers, G. Schönhense, U. Heinzmann, H. P. Oepen, K. Hünlich, J. Kirschner, and G. Borstel, Phys. Rev. Lett. 52, 1559 (1984).
- [20] Ch. Heckenkamp, A. Eyers, F. Schäfers, G. Schönhense, and U. Heinzmann, Nucl. Instrum. Methods Phys. Res., Sect. A 246, 500 (1986); design: K. Jost, J. Phys. E 12, 1006 (1979).
- [21] K. Kern, R. David, R. L. Palmer, and G. Comsa, Phys. Rev. Lett. 56, 620 (1986).
- [22] Ch. Heckenkamp, F. Schäfers, G. Schönhense, and U. Heinzmann, Phys. Rev. Lett. 52, 421 (1984); Z. Phys. D 2, 257 (1986).
- [23] F. Meier and D. Pescia, in *Optical Orientation*, edited by F. Meier and B. P. Zakharchenya (North-Holland, Amsterdam, 1984), p. 346ff.
- [24] V. Saile, M. Skibowski, W. Steinmann, P. Gürtler, E. E. Koch, and A. Kozevnikov, Phys. Rev. Lett. 37, 305 (1976).
- [22] J. Stapelfeldt, J. Wörner, and T. Möller, Phys. Rev. Lett. 62, 98 (1989); J. Stapelfeldt, J. Wörner, G. Zimmerer, and T. Möller, Z. Phys. D 12, 435 (1989).
- [26] J. E. Cunningham, D. Greenlaw, J. L. Erskine, R. P. Layton, and C. P. Flynn, J. Phys. F 7, L281 (1977); C. P. Flynn, Phys. Rev. Lett. 57, 267 (1986).

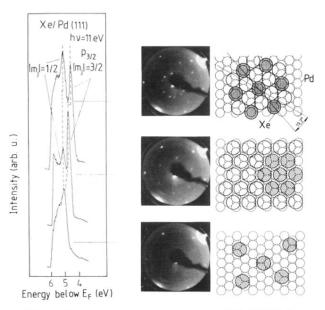


FIG. 1. Photoelectron intensity spectra of Xe/Pd(111) taken at hv=11 eV (left-hand panel), LEED patterns (center panels), and compatible structures (right-hand panels) for (a) the dilute phase, (b) the $(\sqrt{3} \times \sqrt{3})R30^{\circ}$ structure, and (c) the $(\sqrt{7} \times \sqrt{7})R19.2^{\circ}$ structure.